[23] S. Lipsky, J. Chem. Phys. **38**, 2786 (1963).
[24] R. B. Cundall and P. A. Griffiths, J. Phys. Chem. **69**, 1866 (1965).
[25] J. T. Dubois and F. Wilkinson, J. Chem. Phys. **38**, 2541 (1963).
[26] D. S. Mc. Clure, J. Chem. Phys. **17**, 905 (1949).
[27] W. G. Hekstroeter, A. A. Lamola, and G. S. Hammond, J. Am. Chem. Soc. **86**, 4537 (1964).
[28] R. S. H. Liu and J. R. Edman, J. Am. Chem. Soc. **90**, 213 (1968).
[29] A. Morikawa and R. J. Cvetanovic, Can. J. Chem. **46**, 1813 (1968).
[30] S. J. Rzad, R. H. Schuler, and A. Hummel, J. Chem. Phys. **51**, 1369 (1969).
[31] Evidence has been obtained in this laboratory that aromatic ketones such as valerophenone react with electrons.

THE JOURNAL OF CHEMICAL PHYSICS VOLUME 53, NUMBER 9 1 NOVEMBER 1970

Vibrational Exciton Density of States in Solid Benzene*

J. C. LAUFER† AND R. KOPELMAN
Department of Chemistry, University of Michigan, Ann Arbor, Michigan 48104

(Received 11 May 1970)

Computer-aided calculations, based on experimentally-fitted pairwise interaction terms, give the complete exciton density-of-states profile for the entire Brillouin zone. The restricted Frenkel model, with short-range interactions, is the key assumption. Results are given and discussed for the out-of-plane a_{2u} normal mode ν_{11} (C_6H_6 and C_6D_6), for $\nu_{12}(b_{1u})$, and for $\nu_{15}(b_{2u})$. The wide range of parameters used makes this investigation pertinent to other vibrational and electronic exciton bands of benzene and any other molecular crystal with the same interchange symmetry. Also, Van Hove singularities are found to be more important for symmetry-based critical points than for "accidental" critical points. Present-day experimental and theoretical intermolecular excitation exchange interaction terms are compared.

INTRODUCTION

The usual experimental investigations of the vibrational and electronic states of molecular crystals involve the observations of the infrared or ultraviolet transitions between the ground and excited states of the crystal. Since the ground state is characterized by the reduced wave vector $\mathbf{k}=0$, the general crystal selection rule for this region, $\Delta\mathbf{k}\cong 0$, restricts the optically allowed transitions to those involving only the $\mathbf{k}\cong 0$ states of the vibrational or electronic exciton band. Recently, however, the study of the band contours of carefully selected "hot-band" transitions in crystals of benzene and naphthalene have led to the observation of the density-of-states distribution of the entire exciton band of the first excited singlet states of these systems.[1] These band profiles were then compared to theoretically calculated density-of-states distributions based on independent empirical data. No vibrational exciton bands in molecular crystals have yet been observed experimentally, but we have attempted to predict the band shape of some of the benzene vibrational excitons by applying the same theoretical formalism used to calculate the electronic exciton bands. The restricted Frenkel model used here[2] is applicable not only to many vibrational excitons, but also to all electronic Frenkel exciton states that are not associated with strong transition dipole moments.[3] It is particularly applicable to triplet exciton bands.[4]

Another aim of this investigation was to follow the changes in a density-of-states function with changes in pairwise interaction parameters, within the restricted Frenkel exciton theory. A large number of computations have been collected (only a few shown here), providing some insight into the nature of these relationships. Another point of interest has been the role of critical points in restricted Frenkel density-of-states functions. The computed curves are also of interest because they encourage experiments designed to investigate the density-of-states function in the liquid as well as the solid state.

THEORY

The energy distribution of the density of exciton states of a molecular crystal can be easily determined once the eigenvalue problem for the exciton band has been solved. For molecular crystals such as benzene and naphthalene, Frenkel exciton theory and the assumption of pairwise molecular interactions are the standard approaches for obtaining exciton energies.[5,6] References 1 and 6 contain the formalism for deriving the matrix elements for the excited state of crystalline benzene. These matrix elements, $L_{qq'}{}^{f}(\mathbf{k})$, defined by Eq. (7) of Ref. 6, correspond to the excited state of the molecule, whether electronic or vibrational:

$$L_{qq'}{}^{f}(\mathbf{k}) = \langle \phi_q{}^{f}(\mathbf{k}) \mid H \mid \phi_{q'}{}^{f}(\mathbf{k}) \rangle$$
$$= \sum_{n'=1}^{N/h} [\exp(i\mathbf{k})\cdot(\boldsymbol{\tau}_{q'}-\boldsymbol{\tau}_q)]$$
$$\times[\exp(i\mathbf{k})\cdot(\mathbf{r}_{n'}-\mathbf{r}_n)]\int \phi_{nq}{}^{f*} H \phi_{n'q'}{}^{f} dR. \quad (1)$$

In general, the diagonal element $L_{qq}{}^{f}(\mathbf{k})$ is not equal to the diagonal element $L_{q'q'}{}^{f}(\mathbf{k})$ because the dot products of a given $\mathbf{k}$ with the vectors $(\mathbf{r}_n+\boldsymbol{\tau}_q)$ of sublattice q are different[2,3,5] from the dot products with the vectors $(\mathbf{r}_n+\boldsymbol{\tau}_{q'})$, associated with sublattice q'.

However, in the restricted Frenkel limit,[2,3]

$$L_{qq}{}^{f}(\mathbf{k}) = L_{q'q'}{}^{f}(\mathbf{k}). \tag{2}$$

This limit is justified for the benzene crystal if, for example, the summation in Eq. (1) is truncated after summing over the 12 nearest interchange equivalent neighbors and the 8 nearest translationally equivalent neighbors along the **a**, **b**, and **c** axes. When Eq. (2) is invoked,[2,6] the eigenvalues of the secular determinant, relative to the band center, can be written as

$$E^{f\alpha}(\mathbf{k}) = \sum_{q=I}^{h} a_q{}^{\alpha} L_{Iq}{}^{f}(\mathbf{k}), \tag{3}$$

where the $a_q{}^{\alpha}$'s are coefficients corresponding to the character elements of the αth irreducible representation of an interchange group **G** of order h. **G** is a group whose h elements comprise the symmetry operations which generate the h molecules of the primitive cell from one arbitrary molecule[7] [labeled $q=I$ in Eq. (3)].

For benzene, we have chosen a $\mathbf{D}_2$ interchange group[7] to generate the four sets of $E^{f\alpha}(\mathbf{k})$. These correspond to the four branches of an exciton band in benzene. Equation (3) for benzene, after substituting Eq. (1) for $L_{Iq}{}^{f}(\mathbf{k})$ and truncating the summation after the nearest translationally equivalent neighbors, can be written[1]

$$\begin{aligned} E^{f\alpha}(\mathbf{k}) = {} & 2M_a \cos(k_a a) + 2M_b \cos(k_b b) + 2M_c \cos(k_c c) \\ & + 4a_{\mathrm{II}}{}^{\alpha} M_{\mathrm{I\,II}} \cos(k_a \tfrac{1}{2} a) \cos(k_b \tfrac{1}{2} b) \\ & + 4a_{\mathrm{III}}{}^{\alpha} M_{\mathrm{I\,III}} \cos(k_b \tfrac{1}{2} b) \cos(k_c \tfrac{1}{2} c) \\ & + 4a_{\mathrm{IV}}{}^{\alpha} M_{\mathrm{I\,IV}} \cos(k_a \tfrac{1}{2} a) \cos(k_c \tfrac{1}{2} c), \end{aligned} \tag{4}$$

where the notation is that of Ref. 1 [Eq. (3)]. The density-of-states function can be calculated directly from Eq. (4) simply by counting the number of states having energies E' between E and $E+\Delta E$. The plot of this number $\rho(E')$ versus E' is then assumed to be the exciton band profile.[6]

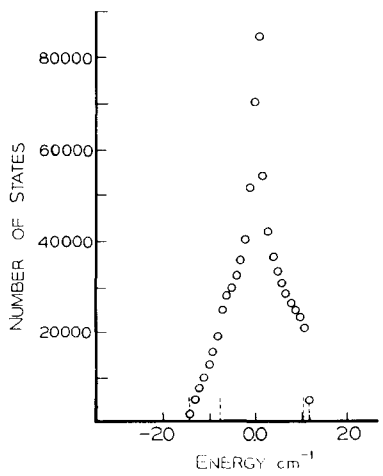

FIG. 1. $a_{2u}(\nu_{11})$ exciton band. $M_a=M_b=M_c=0$, $M_{\mathrm{I\,II}}=-0.4$, $M_{\mathrm{I\,III}}=2.8$, $M_{\mathrm{I\,IV}}=0.5$. Resolution is 1 cm^{-1}.

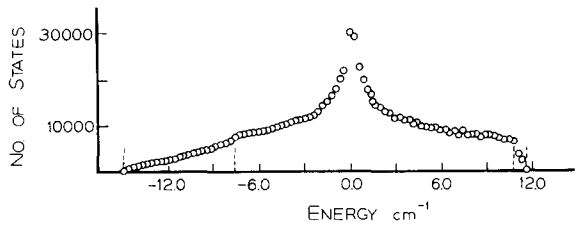

FIG. 2. $a_{2u}(\nu_{11})$ exciton band. $M_a=M_b=M_c=0$, $M_{\mathrm{I\,II}}=-0.4$ $M_{\mathrm{I\,III}}=2.8$, $M_{\mathrm{I\,IV}}=0.5$ Resolution is 0.3 cm^{-1}.

CALCULATIONS AND RESULTS

The calculation of the band profiles from Eq. (4) involved a total of 864 000 energy states arising from the choice of a crystal of that number of molecules. The density of the energy states was then determined to a resolution of 1 cm^{-1} for the C_6H_6 ν_{11} bands, 0.3 cm^{-1} for the C_6D_6 ν_{11} and the C_6H_6 ν_{12} bands, and 0.1 cm^{-1} for the C_6H_6 ν_{15} band. It was determined that at these resolutions and with the number of states chosen, the "noise" in the band profile is too low to be detected. All the features displayed by the band contours are thus believed to be real to within the approximation that the band profile is determined by the density-of-states function and Eq. (4). As mentioned above, Eq. (4) is derived from Eq. (1) in the restricted Frenkel limit, i.e., by truncating the pairwise lattice sum after the eight nearest translationally equivalent neighbors. In view of the fact that the intermolecular forces in the benzene crystal are relatively short-range and the values of even M_a, M_b, and M_c are claimed to be close to zero,[8–10] the truncation probably does not introduce any measurable error in the energies of the exciton states. The shape and width of the exciton bands are determined entirely by the values of the interaction constants. It can be seen from Eq. (4) that the larger the size of these constants, the wider the band will be.

The band profiles derived from Eq. (4) are shown in Figs. 1–11. Figures 1–7 are various band contours for the C_6H_6 vibrational a_{2u} (ν_{11}) exciton band. Depending on the choice of data and the scale on which the density of states is plotted, the ν_{11} band varies in appearance from figure to figure. Figure 1 shows the band profile, plotted at a resolusion of 1 cm^{-1}, obtained from the experimental work of Bernstein and Robinson on neat and mixed crystals of benzene.[11] The band center, adjusted to zero energy, is at 696.9 cm^{-1}, and is taken to be the ideal mixed-crystal value. The four dotted lines at -14.8, -7.6, 10.8, and 11.6 cm^{-1} are the values of the four Davydov components, three of which have been observed in neat-crystal experiments, while the fourth (11.6 cm^{-1}) was calculated from the other three

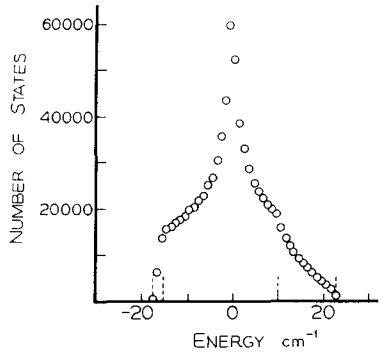

FIG. 3. $a_{2u}(\nu_{11})$ exciton band. $M_a=M_b=M_c=0$, $M_{\text{I II}}=0.7$ $M_{\text{I III}}=4.1$, $M_{\text{I IV}}=0.9$.

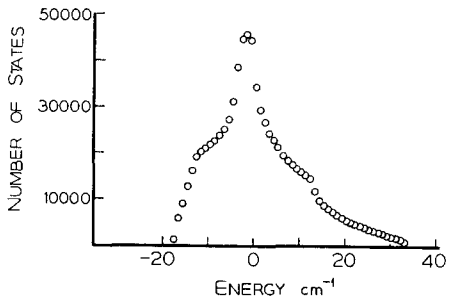

FIG. 4. $a_{2u}(\nu_{11})$ exciton band. $M_a=1$, $M_b=0$, $M_c=1$, $M_{\text{I II}}=1.2$, $M_{\text{I III}}=4.6$, $M_{\text{I IV}}=1.4$.

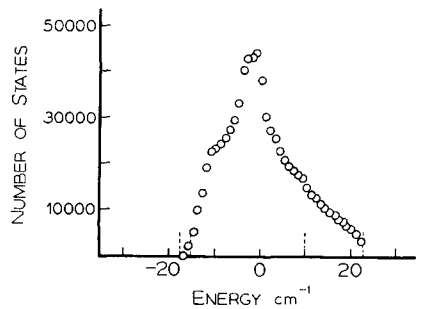

FIG. 5. $a_{2u}(\nu_{11})$ exciton band. $M_a=-1$, $M_b=0$, $M_c=1$, $M_{\text{I II}}=0.7$, $M_{\text{I III}}=4.1$, $M_{\text{I IV}}=0.9$.

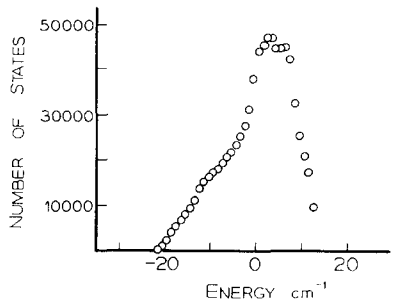

FIG. 6. $a_{2u}(\nu_{11})$ exciton band. $M_a=-2$, $M_b=0$, $M_c=-2$, $M_{\text{I II}}=-0.3$, $M_{\text{I III}}=3.1$, $M_{\text{I IV}}=-0.1$.

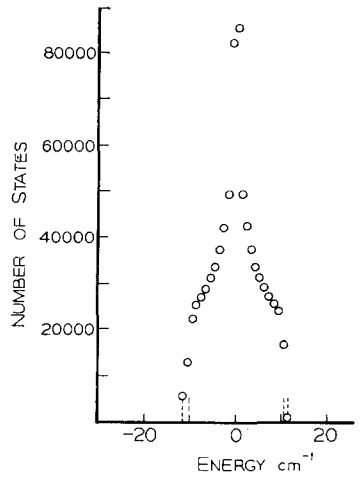

FIG. 7. $a_{2u}(\nu_{11})$ exciton band. $M_a=M_b=M_c=0$, $M_{\text{I II}}=-0.1$ $M_{\text{I III}}=2.7$, $M_{\text{I IV}}=0.2$.

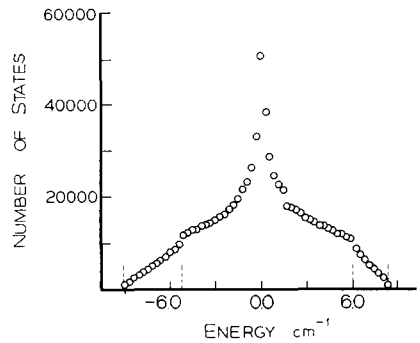

FIG. 8. C_6D_6 $a_{2u}(\nu_{11})$ exciton band. $M_a=M_b=M_c=0$, $M_{\text{I II}}=-0.4$ $M_{\text{I III}}=1.8$, $M_{\text{I IV}}=0.1$.

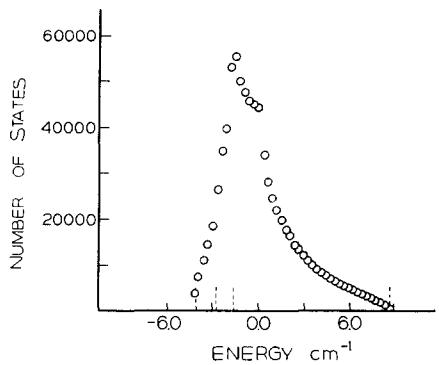

FIG. 9. $b_{1u}(\nu_{12})$ exciton band. $M_a=M_b=M_c=0$, $M_{\text{I II}}=0.89$, $M_{\text{I III}}=0.75$, $M_{\text{I IV}}=0.54$.

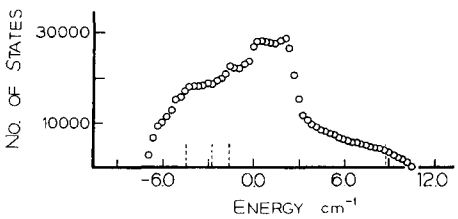

FIG. 10. $b_{1u}(\nu_{12})$ exciton band. $M_a=-1.5$, $M_b=0.75$, $M_c=0.75$ $M_{\text{I II}}=0.89$, $M_{\text{I III}}=0.75$, $M_{\text{I IV}}=0.54$.

with the aid of mixed-crystal data. It was assumed, in accordance with indirect experimental evidence,[11,12] that this band has a translational shift of 0 cm^{-1}, and that the three interaction constants, M_a, M_b, and M_c, involving translationally equivalent molecules, are each 0.0 cm^{-1} in value.[8-11] The interchange equivalent interaction constants, $M_{I\,II}$, $M_{I\,III}$, and $M_{I\,IV}$ were then calculated from Eq. (4), in which $\mathbf{k}$ was set equal to zero.

Figure 2 shows the band in Fig. 1 plotted at a resolution of 0.3 cm^{-1}. The 864 000 energy states used in the calculation are now distributed in a finer mesh, and as a result, statistical "noise" appears on the high-energy side of the band. This "noise" could be eliminated by increasing the number of states used in the calculation. One advantage of using a higher resolution plot such as that in Fig. 2 is that the shape of the band is easy to see. The basic features in this band are the high and low frequency edges, at -14.8 and 11.6 cm^{-1}, respectively, the peak at the band center, and the two abrupt changes in slope at -7.6 and 10.8 cm^{-1}. Each of these details can be explained in terms of Van Hove singu-

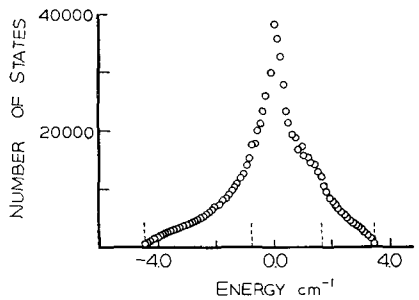

FIG. 11. $b_{2u}(\nu_{15})$ exciton band. $M_a=M_b=M_c=0$, $M_{I\,II}=0.12$, $M_{I\,III}=0.34$, $M_{I\,IV}=-0.64$.

larities: those critical points where the gradient of a branch equals zero.[13] In our notation

$$\nabla_k E^{f\alpha}(\mathbf{k})=0. \tag{5}$$

By redefining the angular variables in Eq. (4) such that

$$k_a a=k_x, \qquad k_b b=k_y, \qquad k_c c=k_z, \tag{6}$$

the critical points are found[13] by solving the three simultaneous equations

$$\partial E^{f\alpha}(\mathbf{k})/\partial k_x=\partial E^{f\alpha}(\mathbf{k})/\partial k_y=\partial E^{f\alpha}(\mathbf{k})/\partial k_z=0. \tag{7}$$

We simplified the problem of solving the simultaneous equations by setting the "translational" interaction constants, M_a, M_b, M_c, equal to 0.0 cm^{-1} and thus reduced Eq. (4) to

$$\begin{aligned}E^{f\alpha}(\mathbf{k})=&\,4a_{II}{}^{\alpha}M_{I\,II}\cos(\tfrac{1}{2}k_x)\cos(\tfrac{1}{2}k_y)\\&+4a_{III}{}^{\alpha}M_{I\,III}\cos(\tfrac{1}{2}k_y)\cos(\tfrac{1}{2}k_z)\\&+4a_{IV}{}^{\alpha}M_{I\,IV}\cos(\tfrac{1}{2}k_x)\cos(\tfrac{1}{2}k_z).\end{aligned} \tag{8}$$

The solutions to Eq. (7) can now be found in closed

TABLE I. Van Hove singularities for benzene excitons.

Necessary conditions	Branch	k_x	k_y	k_z	$E^{f\alpha}(\mathbf{k})$
	A_u	0	0	0	$4(M_{I\,II}+M_{I\,III}+M_{I\,IV})$
	B_{1u}	0	0	0	$4(M_{I\,II}-M_{I\,III}-M_{I\,IV}$
	B_{2u}	0	0	0	$4(-M_{I\,II}+M_{I\,III}-M_{I\,IV})$
	B_{3u}	0	0	0	$4(-M_{I\,II}-M_{I\,III}+M_{I\,IV})$
	All	π	π	π	0
$\lvert M_{I\,III}\rvert\geq\lvert M_{I\,II}\rvert,\lvert M_{I\,IV}\rvert$	All	0	$2\arccos(-a_{IV}M_{I\,IV}/a_{III}M_{I\,III})$	$2\arccos(-a_{II}M_{I\,II}/a_{III}M_{I\,III})$	$-4M_{I\,II}M_{I\,IV}/M_{I\,III}$
$\lvert M_{I\,IV}\rvert\geq\lvert M_{I\,II}\rvert,\lvert M_{I\,III}\rvert$	All	$2\arccos(-a_{III}M_{I\,III}/a_{IV}M_{I\,IV})$	0	$2\arccos(-a_{II}M_{I\,II}/a_{IV}M_{I\,IV})$	$-4M_{I\,II}M_{I\,III}/M_{I\,IV}$
$\lvert M_{I\,II}\rvert\geq\lvert M_{I\,III}\rvert,\lvert M_{I\,IV}\rvert$	All	$2\arccos(-a_{III}M_{I\,III}/a_{II}M_{I\,II})$	$2\arccos(-a_{IV}M_{I\,IV}/a_{II}M_{I\,II})$	0	$-4M_{I\,III}M_{I\,IV}/M_{I\,II}$

TABLE II. Critical points in benzene vibrational excitons.

Vibration	$M_{I\,II}$ (cm^{-1})	$M_{I\,III}$ (cm^{-1})	$M_{I\,IV}$ (cm^{-1})	Branch	k_x	k_y	k_z	$E(cm^{-1})$
C_6H_6 ν_{11}	−0.4	2.8	0.5	A_u	0	0	0	11.6
(Fig. 1, 2)				B_{1u}	0	0	0	−14.8
				B_{2u}	0	0	0	10.8
				B_{3u}	0	0	0	−7.6
				All	π	π	π	E0.0
				All	0	2 arccos[(±0.5)/2.8]	2 arccos[(±0.4)/2.8]	0.3
C_6H_6 ν_{11}	0.7	4.1	0.9	A_u	0	0	0	22.8
(Fig. 3)				B_{1u}	0	0	0	−17.2
				B_{2u}	0	0	0	10.0
				B_{3u}	0	0	0	−15.6
				All	π	π	π	0.0
				All	0	2 arccos[(±0.9)/4.1]	2 arccos[(±0.7)/4.1]	−0.6
C_6D_6 ν_{11}	−0.4	1.8	0.1	A_u	0	0	0	6.0
(Fig. 8)				B_{1u}	0	0	0	−9.2
				B_{2u}	0	0	0	8.4
				B_{3u}	0	0	0	−5.2
				All	π	π	π	0.0
				All	0	2 arccos[(±0.1)/1.8]	2 arccos[(±0.4)/1.8]	0.1
C_6H_6 ν_{11}	−0.1	2.7	0.2	A_u	0	0	0	11.2
(Fig. 7)				B_{1u}	0	0	0	−12.0
				B_{2u}	0	0	0	10.4
				B_{3u}	0	0	0	−9.6
				All	π	π	π	0.0
				All	0	2 arccos[(±0.2)/2.7]	2 arccos[(±0.1)/2.7]	0.03
C_6H_6 ν_{15}	0.12	0.34	−0.64	A_u	0	0	0	−0.72
(Fig. 11)				B_{1u}	0	0	0	1.68
				B_{2u}	0	0	0	3.44
				B_{3u}	0	0	0	−4.40
				All	π	π	π	0.00
				All	2 arccos[(±0.34)/0.64]	0	2 arccos[(±0.12)/0.64]	0.25
C_6H_6 ν_{12}	0.89	0.75	0.54	A_u	0	0	0	8.72
(Fig. 9)				B_{1u}	0	0	0	−1.60
				B_{2u}	0	0	0	−2.72
				B_{3u}	0	0	0	−4.40
				All	π	π	π	0.00
				All	2 arccos[(±0.75)/0.89]	2 arccos[(±0.54)/0.89]	0	−1.82

TABLE III. Interaction constants of C_6H_6 ν_{11} band obtained from data of various investigators.

Source	Band center (cm^{-1})	$M_{I\,II}$ (cm^{-1})	$M_{I\,III}$ (cm^{-1})	$M_{I\,IV}$ (cm^{-1})	
Bernstein and Robinson[a]	696.9	−0.4	2.8	0.5	"Experimental"
Hollenberg and Dows[b]	697	0.7	4.1	0.9	"Experimental"
Harada and Shimanouchi[c]	695.4	−0.1	2.7	0.2	Calculated
Rich and Dows[d]	695.5	0.0	4.2	0.38	Calculated

[a] Reference 11.
[b] Reference 14.
[c] Reference 8.
[d] Reference 9.

form. However, many of the possible roots are physically meaningless and have to be excluded. We have listed the acceptable roots and their energy expressions in Table I and calculated these energies for the various vibrational excitons in Table II.

The critical points of the band derived from the data of Bernstein and Robinson are given in the first entry of Table II. It is apparent that the four Davydov components and the corner of the Brillouin zone at $(\pi\pi\pi)$ are the critical points which are visible in the density-of-states function. The singularity at 0.3 cm^{-1} is not visible, possibly because it is overlapped by the 0.0-cm^{-1} peak of the critical point at $(\pi\pi\pi)$. To within the approximation that the translationally equivalent molecules' pairwise interaction constants are zero, the four branches stick not only at $(\pi\pi\pi)$, but also at a second point in the Brillouin zone which is located close to the center of one of the zones faces. This critical point is determined by the values of the interaction constants and is not a point of special symmetry as are the other five points listed in Table I. The degeneracy of the branches at this point is an artifact of the simplified dispersion relation [Eq. (8)] used to describe the benzene vibrational excitons, and is expected to disappear if a more general dispersion relation is used. On the other hand, the four branches must all, for symmetry reasons, have the same energy values at the point $(\pi\pi\pi)$.

When all the bands listed in Table II are analyzed for features which can be correlated with their Van Hove singularities, it is seen that almost all the features can be explained in terms of symmetry-based critical points, i.e., the four Davydov components and the critical point at $(\pi\pi\pi)$. The accidental (nonsymmetry-based) singularity does not appear clearly in any of the bands. Had the bands shown been calculated from a finer mesh in the Brillouin zone, this singularity would have had to appear; but in view of the present low resolution of any experimentally observed density-of-states functions, and the fact that no vibrational density-of-states bands have been observed yet, it is not of immediate importance to do more extensive (i.e., finer mesh) calculations. Nor do the empirical M's or equation (8) justify such calculations.

Figure 3 shows the ν_{11} exciton band calculated by using the slightly older neat and mixed crystal data of Hollenberg and Dows.[14] The large difference in width between the bands in Figs. 2 and 3 is indicative of the experimental difficulties in getting precise vibrational exciton spectra in the benzene system. It should be noted that the experiments by Hollenberg and Dows were conducted with emphasis on intensity measurements. On the other hand, they agree better with the inferred, tentative resonance pair data[12] than those of Bernstein and Robinson.[11] The theoretical studies of the benzene vibrations[8,9] give still different band profiles for the ν_{11} mode. Table III lists the values of the M's derived from both the experimental and the theoretical results for this vibration.

Figures 4–6 demonstrate the effect on the band shape when M_a, M_b, and M_c were allowed to have nonzero values. Once the values of the "translational" interaction constants were chosen, the "interchange" interaction constants were obtained by the same method described before. Figure 7 is the band profile of the ν_{11} band using the interaction constants derived from the Davydov components calculated by Hirada and Schimanouchi.[8,12] Since these calculated Davydov components give a narrower exciton splitting than is observed experimentally, the band in Fig. 7 is narrower than the band in Fig. 1. The unusual height of the peak in Fig. 7 is simply a consequence of squeezing the exciton states into a narrow energy range. Figure 8 is a band profile of the ν_{11} vibration for the perdeuterobenzene crystal.[11] The zero values for M_a, M_b, and M_c were assumed.

Figures 9 and 10 show ν_{12} band profiles. In Fig. 10, unrealistically large values of M_a, M_b, and M_c were chosen to demonstrate the sensitivity of the band shape to the size of the interaction constants. Figure 11 is the band profile for the ν_{15} band.[11] As in previous cases, the values of M_a, M_b, and M_c were assumed to be zero. It should be noted that the critical points, as given in Table II, apply to most, but not all figures.

DISCUSSION

The band structures displayed in Figures 1–11 can be viewed as an empirical computer study, relating parameters to band shapes within the restricted Frenkel theory. By looking at these figures, as well as at about 50 more figures of the same kind, we can suggest that large M_a, M_b, or M_c parameters result in at least one "plateau" (see Fig. 10). Obviously such parameters also cause the band to "spill" outside the outer Davydov components, often only on one side. Another observation is that the symmetry-based critical points usually correspond to clearly visible Van Hove singularities in the density-of-states functions, even with coarse-mesh calculations. In bands derived from Eq. (8) there are no clearly visible Van Hove singularities corresponding to the accidental critical points. These singularities would obviously appear[13] in a fine-mesh calculation. However, it is doubtful whether fine-mesh computations, such as those of Sommer and Jortner[13] for electronic states, are presently justified in view of both the crudeness of the available parameters, experimental or theoretical, and the truncated dispersion relations used.

It should be noted that in the restricted Frenkel approach the band shape (density of states) is essentially determined by a small number of nearest and near-neighbor interactions. This dependence on only a few interactions has been demonstrated to be applicable for certain electronic exciton bands[1,6] and should apply even more so to vibrational exciton bands where it is well known that the magnitude of the intermolecular interactions (involving the excited state) falls off drastically with distance.[15] Thus, both the use of the restricted Frenkel model *and* the additional truncations [Eqs. (4) and (8)] seem to be fully justified here. It may be noted that even for the intense a_{2u} band the dipole–dipole interactions are about one order of magnitude too small to account for the band (see Appendix). For "forbidden" bands, like ν_{15}, these dipole–dipole interactions vanish if free benzene molecules are considered, or are negligible if site-distorted molecules are considered.

No vibrational exciton band structures have been observed experimentally so far. Work in this direction is now in progress in our laboratory. A preliminary investigation of the a_{2u} *liquid* exciton band[16] reveals an *exciton* band shape not very different from the ones given in Figs. 1–3.

The calculations by Harada and Schimanouchi[8] (Fig. 7) and by Rich and Dows[9] seem to be in the right ballpark, but do not agree in detail with our "experimentally derived" bands. However, in view of the experimental difficulties mentioned above, it may be too early to draw any definite conclusions about the significance of this discrepancy.

SUMMARY

Density-of-state functions are represented for four vibrational excitons. These are based on experimental data combined with the restricted Frenkel theory. Symmetry-based critical points play a major role in these band shapes. Present-day experimental techniques and theoretical models are compatible (i.e., equally crude).

APPENDIX

The magnitude of the dipole–dipole interactions in a vibrational exciton can be estimated by obtaining the value of the dipole transition moment from the absolute intensity of the vibration in an ideal mixed crystal, and then using this transition moment with dipole–dipole lattice sums to calculate the Davydov components of the exciton band. Hollenberg and Dows[17] report the absolute absorption intensity of the a_{2u} vibration of 5.03% C_6H_6 in a C_6D_6 lattice to be 7800 ± 1200 darks. For a vibrational transition from the ground to first excited state, the relationship between the absolute absorption intensity $\bar{A}_{01}$ and $|\mu_{01}|^2$, the square of the dipole transition moment, is given by[18]

$$\bar{A}_{01}=[8\pi^3N/3hc(1000)]\bar{\nu}_{01}|\mu_{01}|^2. \qquad \text{(A1)}$$

In Eq. (14), $\bar{\nu}_{01}$ is the ideal-mixed-crystal frequency of the transition in wavenumbers (697 cm^{-1} for ν_{11}), N is Avogardo's number, h is Planck's constant, and c is the speed of light.

$|\mu_{01}|^2$ for ν_{11} is found to be 4.4×10^{-38} erg·cm³. Dipole–dipole lattice sums for crystalline benzene are given by Thirunamachandran in his Ph.D. thesis.[19] The sums are in units of $cm^{-1}\cdot Å^{-2}$, which means that the dipole moments must be translated into units of angstroms. The conversion is as follows:

$$\begin{aligned}|\mu_{01}|^2&=4.4\times10^{-38}\ \text{erg}\cdot\text{cm}^3\\&=4.4\times10^{-38}\ \text{esu}^2\cdot\text{cm}^2\\&=[(4.4\times10^{-38})(10^{16})/(4.8\times10^{-10})^2]\ Å^2\\&=1.92\times10^{-3}\ Å^2. \qquad \text{(A2)}\end{aligned}$$

The lattice sums are given for the dipole–dipole interactions between different sublattices, so it is possible to calculate from them the positions of the Davydov components relative to the band center:

A_u, $-2.4\ cm^{-1}$; B_{1u}, $3.1\ cm^{-1}$;

B_{2u}, $-1.2\ cm^{-1}$; B_{3u}, $0.5\ cm^{-1}$.

The total bandwidth in the dipole–dipole approximation is thus 5.5 cm^{-1}. Figure 3, which is derived from the data of Dows and Hollenberg, shows this band, calculated from experimental observation of three Davydov components and mixed-crystal spectra, to be 40 cm^{-1} in width. In the above calculation no retardation effects were included. The latter may even cancel part of the nonretarded terms. It is therefore concluded that the major contribution to the a_{2u} exciton bandwidth comes from short-range contributions.

This conclusion is confirmed by the observation of resonance pairs (see "Note added in proof" of Ref. 12).

* Supported by PHS Grant NB-08116.
† Supported by PHS postdoctoral fellowship 1-F02-NB-43, 931.

[1] S. D. Colson, D. M. Hanson, R. Kopelman, and G. W. Robinson, J. Chem. Phys. **48,** 2215 (1968).

[2] S. D. Colson, R. Kopelman, and G. W. Robinson, J. Chem. Phys. **47,** 27 (1967); **47,** 5462 (1967).

[3] R. Kopelman and J. C. Laufer, Natl. Bur. Std. (U.S.), Spec. Publ. **323** (1970).

[4] R. H. Clarke and R. M. Hochstrasser, J. Chem. Phys. **49,** 3313 (1968); **46,** 4532 (1967).

[5] R. S. Knox, *Theory of Excitons* (Academic, New York, 1963), Chap. II.

[6] E. R. Bernstein, S. D. Colson, R. Kopelman, and G. W. Robinson, J. Chem. Phys. **48,** 5596 (1968).

[7] R. Kopelman, J. Chem. Phys. **47,** 2631 (1967).

[8] I. Harada and T. Shimanouchi, J. Chem. Phys. **44,** 2016 (1966).

[9] N. Rich and D. A. Dows, Mol. Cryst. **5,** 111 (1968).

[10] E. R. Bernstein, Ph.D. thesis, California Institute of Technology, 1968. See also E. R. Bernstein, J. Chem. Phys. **52,** 4701 (1970) (appeared after the completion of our work).

[11] E. R. Bernstein and G. W. Robinson, J. Chem. Phys. **49,** 4962 (1968). There are some arithmetical mistakes in Table III of this paper involving signs and designations of M terms. These have been corrected according to their Tables I and II.

[12] R. Kopelman, J. Chem. Phys. **47,** 3227 (1967). *Note added in proof:* The resonance pair feature (693.5 cm^{-1}) assigned in this reference was assigned as the natural abundance $^{13}C^{12}C_5H_6$ isolated guest band (694.1 cm^{-1}) by E. R. Bernstein, J. Chem. Phys. **50,** 4842 (1969). However, our recent calculations show that the isotope shift is only 0.3 to 0.4 cm^{-1} (not 3 to 4 cm^{-1}), in agreement with the 0 ± 0.3 cm^{-1} experimental gas phase shift reported by S. Brodersen, J. Christoffersen, B. Bak, and J. T. Nielsen, Spectrochim. Acta **21,** 2077 (1965). The same attitude as ours is also taken in a very recent paper by M. P. Marzocchi, H. Bonadeo, and G. Taddei, J. Chem. Phys. **53,** 867 (1970). Furthermore, the assignment of the exciton components in the latter reference agrees with the older Hollenberg–Dows–Kopelman assignment rather than with that of Ref. 11, i.e., preferring Fig. 3 rather than Fig. 1 as the "closest" density of states for the a_{2u} band.

[13] J. M. Ziman, *Theory of Solids* (Cambridge U. P., Cambridge, England, 1964), p. 46; see also B. S. Sommer and J. Jortner, J. Chem. Phys. **50,** 839 (1969).

[14] The values for the interaction constants are taken from Ref. 12, which derived these values from J. L. Hollenberg and D. A. Dows, J. Chem. Phys. **37,** 1300 (1962); **39,** 495 (1963).

[15] In explaining vibrational exciton splittings, intermolecular and interatomic forces that have exponential and r^{-6} (or r^{-12} and r^{-6}) dependence are generally assumed. Electronic intermolecular forces are often assumed to be, at least in part, of a dipole–dipole (r^{-3}) nature for singlet electronic excitons.

[16] H. K. Hong and R. Kopelman (unpublished data).

[17] J. L. Hollenberg and D. A. Dows, J. Chem. Phys. **29,** 495 (1963).

[18] G. M. Barrow, *Introduction to Molecular Spectroscopy* (McGraw-Hill, New York, 1962), p. 77.

[19] T. Thirunamachandran, Ph.D. thesis, University of London, 1961.

THE JOURNAL OF CHEMICAL PHYSICS VOLUME 53, NUMBER 9 1 NOVEMBER 1970

Theoretical Study of H_2^+ Ground Electronic State Spectroscopic Properties*

CHARLES L. BECKEL AND BERTLE D. HANSEN III
Department of Physics and Astronomy, The University of New Mexico, Albuquerque, New Mexico 87106
AND
JAMES M. PEEK
Sandia Laboratory, Albuquerque, New Mexico 87115

(Received 1 July 1970)

Born–Oppenheimer and adiabatic vibrational–rotational eigenvalues are determined for the $(1s\sigma_g)\ ^2\Sigma_g^+$ ground state of H_2^+ by a combination of Runge–Kutta and Adams–Moulton numerical techniques. These eigenvalues are believed to be more accurate than any previously reported. Dunham expansions of the potentials are used to determine Born–Oppenheimer and adiabatic spectroscopic constants; the adiabatic constants are considered to be the best set, theoretical or experimental, available for the ground state of H_2^+. The ΔG curve for this state has two points of inflection and a positive curvature tail, presumably to be associated with long-range $1/R^4$ forces in the molecular ion. The B_v curve has a shape similar to the ΔG curve; more striking, inflection points occur at essentially the same values of the vibrational quantum number v. The D_v curve has a negative slope at $v=0$, but rises rapidly near dissociation. The H_v values decrease and become negative at large v values. The sharp rise at high v in $|H_v|$, like that in D_v, is probably due to the dominance of the centrifugal reaction over the true potential at large nuclear separations R.

INTRODUCTION

Practical considerations have prompted study of the hydrogen molecular ion in a number of different contexts; notable examples include the scattering of H_2^+ by a variety of targets[1] and measurement of H_2^+ hyperfine spectra.[2] A few low-lying H_2^+ energy levels have been located experimentally[3] from H_2 Rydberg series limits; several ground-state spectroscopic constants of H_2^+ have been estimated by extrapolation of hydrogen excited-state constants.[4] However, ordinary band spectra from H_2^+ have not as yet been observed. As a consequence, detailed information on the vibrational–rotational structure of H_2^+ provided by high-resolution optical spectroscopy is not available.

The simplicity of H_2^+ places it in a unique role. It alone (along with its isotopic and isoelectronic species) among molecules possesses a fixed nucleus Schrödinger equation that is separable and can be conveniently solved to a predetermined accuracy when only static